Nonthermal optical control of magnetism and ultrafast laser-induced spin dynamics in solids

2007 J. Phys.: Condens. Matter 19 043201

(http://iopscience.iop.org/0953-8984/19/4/043201)

INSTITUTE OF PHYSICS PUBLISHING JOURNAL OF PHYSICS: CONDENSED MATTER

J. Phys.: Condens. Matter **19** (2007) 043201 (24pp) doi:10.1088/0953-8984/19/4/043201

TOPICAL REVIEW

Nonthermal optical control of magnetism and ultrafast laser-induced spin dynamics in solids

Alexey V Kimel[1], Andrei Kirilyuk[1], Fredrik Hansteen[1], Roman V Pisarev[2] and Theo Rasing[1]

[1] IMM, Radboud University Nijmegen, Toernooiveld 1, 6525 ED Nijmegen, The Netherlands
[2] Ioffe Physico-Technical Institute, Polytekhnicheskaya 26, 194021 St-Petersburg, Russia

E-mail: a.kimel@science.ru.nl

Received 3 April 2006, in final form 14 December 2006
Published 12 January 2007
Online at stacks.iop.org/JPhysCM/19/043201

Abstract

Ultrafast laser control of magnetism is one of the most exciting and challenging issues in physics and technology. Such a technique may provide the solution to the need for an ever increasing speed of data storage and manipulation. This review summarizes the recent progress in the study of ultrafast nonthermal effects of light on magnetic materials. Beginning with an introduction, the paper focuses on three main routes for laser control of magnetism. First, it is shown that due to the inverse, opto-magnetic Faraday effect, circularly polarized light may magnetize a medium. Microscopically, this effect is explained in terms of stimulated Raman scattering, where a spin-flip process requires neither annihilation of a photon, nor loss of its angular momentum. The feasibility of the inverse Faraday effect in magnetically ordered materials is demonstrated on the examples of orthoferrites and garnets. In particular, the effect of a 100 fs optical pulse on spins in $DyFeO_3$ is found to be equivalent to an equally short magnetic field pulse up to 1 T. Second, linearly polarized 100 fs laser pulses are shown to create a long-lived modification of the magnetocrystalline anisotropy in magnetic garnets via optically induced electron transfer between nonequivalent ion sites. Third, we show that a combination of two pump pulses and nonthermal effects can lead to coherent control of magnetization dynamics and ultrafast magnetization switching. The review concludes with a summary and an outlook to the feasibility of laser control of magnetism in a broad class of materials.

(Some figures in this article are in colour only in the electronic version)

Contents

1. Introduction

The demand for an ever-increasing speed of information storage and manipulation has triggered an intense search for ways to control the magnetization of a medium by means other than magnetic fields [1–5]. Control of magnetism by light is one of the promising approaches to this problem. This is evidenced by recent experiments, which demonstrate that excitation of a magnetically ordered material with an ultrashort (10^{-13} s and shorter) laser pulse may result in demagnetization [6–16], spin-reorientation [17–19], or even modification of magnetic structure [20, 21], and this all on a timescale of 1 ps or less. Nevertheless, for all the above-mentioned experiments, the observed magnetic changes were a result of laser-induced heating. Due to energy dissipation, light may effectively heat a medium. Since magnetization and constants of magnetic anisotropy are functions of temperature, such a *thermal* load may effectively change these parameters and thus result in demagnetization and spin-reorientation. This thermal origin of spin excitation considerably limits potential applications because the repetition frequency is limited by the cooling time [22]. Moreover, the recording density is seriously limited by heat diffusion. The solution to both these problems could be a *nonthermal* laser control of magnetism.

More than 40 years ago a theoretical analysis, performed by Pitaevskii, showed that circularly polarized light acts on a transparent dispersive medium as an effective magnetic field and this may result in magnetization of the medium [23]. The phenomenon was called the inverse Faraday effect. Soon after the prediction the inverse Faraday effect was observed in paramagnetic solids [24, 25] and in a plasma [26]. These earlier studies demonstrated that excitation of a medium with a circularly polarized laser pulse corresponds to the action of an effective magnetic field. For a 30 ns laser pulse with a fluence of 10^7 W cm^{-2} the strength of the effective magnetic field was as high as 0.01 G. Modern ultrafast laser systems are able to generate pulses shorter than 100 fs (10^{-13} s) and the fluence of the laser excitation may exceed 10^{10} W cm^{-2}. Thus one may expect that a far stronger inverse Faraday effect is feasible with such pulses. Indeed, recent experimental studies of the inverse Faraday effect in plasmas report that circularly polarized light is able to create an axial magnetic field with strength of tens of kilogauss [27].

Despite all these experiments in paramagnetic solids and in plasmas, observation of an ultrafast inverse Faraday effect in magnetically ordered materials remained a challenge for a long time. A few experimental attempts to observe a nonthermal influence of light on metallic magnetic systems with the help of time-resolved magneto-optical measurements have been made [28–30]. It was reported that during the action of a 100 fs laser pulse a large laser-induced magneto-optical signal was observed. However, no impact on the magnetization could be seen after the optical excitation. Thus the ensemble of exchange-coupled spins was not excited and laser control of magnetism was not achieved. The observed ultrafast changes of

the magneto-optical signal during the action of the laser pulse could be explained in terms of nonlinear optical polarizations [31].

An interesting nonthermal approach for optical generation of coherent magnons was recently demonstrated for a Gd surface [32–34]. This material is characterized by a strong coupling between magnons and optical phonons. Therefore, laser excitation of coherent optical phonons effectively leads to coherent spin excitation with a frequency of the optical phonon. However, a complex band structure, a large variety of optically induced electronic transitions [35] and an unfortunate coincidence of several processes in the same narrow time window [15] considerably hampers the analysis of nonthermal effects of light on magnetism in metals.

Novel ferromagnetic III–V semiconducting compounds have recently attracted much attention [36, 37]. In this type of materials the ferromagnetism is mediated by free carriers, and highly effective nonthermal control of the magnetization by light was reported in static measurements [38]. However, these large values of the photoinduced magnetization have not been reproduced or confirmed by dynamic measurements with subpicosecond time resolution [39, 40]. Similar experiments have shown the thermal effects of light on the magnetization [41, 18, 42] and nonthermal effect of light on magnetocrystalline anisotropy [43]. Interpretation of ultrafast magneto-optical response of the ferromagnetic semiconductors is still a subject of debate [44], mainly because the understanding of their electronic, optical, and magnetic properties is limited and even controversial.

Seeking to improve our understanding of ultrafast laser-induced phenomena and searching for nonthermal effects of light on magnetism, dielectrics can be regarded as an alternative approach which possess several significant advantages over metals and semiconductors. The phonon–magnon interaction responsible for thermal effects is much slower in dielectrics than in metals and therefore does not obscure the interpretation of the processes on shorter timescales [45]. Moreover, the electron–spin scattering mechanism proposed in metals [6, 8] does not exist in dielectrics due to the localized nature of their electronic states. Finally, in contrast to the novel magnetic semiconductors, the electronic structure and the optical and magnetic properties of magnetic dielectrics are relatively well understood.

The purpose of this review is to summarize the recent progress in the study of ultrafast nonthermal effects of light on spins in magnetic dielectrics. Based on the analysis of laser-induced spin dynamics we demonstrate the feasibility of ultrafast optical control of both the magnetization and the magnetocrystalline anisotropy. The analysis clearly shows that the mechanisms do not rely on laser-induced heating but have a nonthermal origin. In particular, nonthermal laser control of magnetism is realized via opto- and photo-magnetic effects. Opto-magnetic effects differ from the photo-magnetic ones in that the former are unrelated to the absorption of the light and can be seen most clearly in transparent or weakly absorbing materials [46–48]. The review summarizes important physical aspects of the opto- and photo-magnetic phenomena in dielectrics as well as drawing conclusions about the feasibility of laser control of magnetism in metals and semiconductors.

The paper is organized as follows: section 2 deals with direct nonthermal excitation of the magnetization dynamics on a femtosecond timescale via the inverse Faraday effect. In section 3 the magnetization dynamics obtained via nonthermal laser-induced modification of magnetic anisotropy is discussed. Section 4 describes how a combination of two pump pulses and/or different opto-magnetic effects can lead to a coherent control of magnetization dynamics, and illustrates this on the example of single-pulse ultrafast photo-magnetic switching. The feasibility of laser control of magnetism in metals and semiconductors will be discussed at the end.

2. Inverse Faraday effect and femtosecond opto-magnetism

2.1. Interaction between photons and spins

Can light directly and nonthermally magnetize a medium? The interaction of light with magnetized media is manifested in various magneto-optical phenomena. A good example is the magneto-optical Faraday effect observed as a rotation of the polarization plane θ_F of light transmitted through a magnetic medium,

$$\alpha_F = \frac{\chi}{n}\mathbf{M}\cdot\mathbf{k}, \tag{1}$$

where α_F is the specific Faraday rotation, $\mathbf{M}$ is the magnetization, n is the refractive index, $\mathbf{k}$ is the wavevector of light and χ is the magneto-optical susceptibility, which is a scalar value in isotropic media [49].

Much less known is the inverse, opto-magnetic Faraday effect, where high-intensity laser radiation induces a static $\omega = 0$ magnetization $\mathbf{M}(\mathbf{0})$:

$$\mathbf{M}(\mathbf{0}) = \frac{\chi}{16\pi}[\mathbf{E}(\omega)\times\mathbf{E}(\omega)^*], \tag{2}$$

where $\mathbf{E}(\omega)$ is the electric field of the light wave at frequency ω [23–25]. Therefore, it follows that circularly polarized light at frequency ω should induce a static magnetization $\mathbf{M}(\mathbf{0})$ along the wavevector $\mathbf{k}$. Moreover, right- and left-handed circularly polarized waves should induce magnetizations of opposite sign. Equation (2) can be easily obtained from the thermodynamical definition of the magnetization. In the approximation of a small magnetic field $\mathbf{H}$ one can write $\mathbf{M} = \partial\Phi/\partial\mathbf{H}$, where Φ is the thermodynamical potential and $\mathbf{H}$ is the external magnetic field [50, 51]. It can be shown that for a ferromagnet in the field $\mathbf{E}(\omega)$ of monochromatic light the thermodynamical potential includes a term proportional to $\epsilon[\mathbf{E}(\omega)\times\mathbf{E}(\omega)^*]$, where ϵ is the dielectric permittivity [48]. Since ϵ is a function of magnetic field and $4\pi\chi = \partial\epsilon/\partial\mathbf{H}$, one can see that the term $\epsilon[\mathbf{E}(\omega)\times\mathbf{E}(\omega)^*]$ results in the optically induced magnetization [24].

Equations (1) and (2) show that both direct and inverse Faraday effects are determined by the same magneto-optical susceptibility χ. In particular, in the case of the inverse Faraday effect, χ is the ratio between the induced magnetization and the laser intensity. Therefore, optical control of magnetization is expected to be more efficient in materials with high values of the Faraday rotation per unit magnetization. Another important property of the susceptibility χ is that it has no symmetry restrictions and is thus allowed in all media, regardless of their crystallographic and magnetic structures. Moreover, the inverse Faraday effect, similarly to the direct Faraday effect, does not require absorption at the frequency of light ω.

It must be noted that thermodynamics justifies equation (2) only on a timescale long compared to thermal relaxation times. Therefore, although equation (2) demonstrates the feasibility of the laser induced magnetization, it cannot adequately describe the opto-magnetic phenomenon triggered by a subpicosecond laser pulse. In this case the product $[\mathbf{E}(\omega)\times\mathbf{E}(\omega)^*]$ changes much faster than the characteristic time of phonon–magnon and magnon–magnon interaction. For the description of opto-magnetic phenomena on a subpicosecond timescale one should focus attention on the Hamiltonian itself, not to its thermal average given by the thermodynamical potential. Analysis of the Hamiltonian of the opto-magnetic interaction shows that the product $[\mathbf{E}(\omega)\times\mathbf{E}(\omega)^*]$ acts on magnetic systems as an effective magnetic field [24].

How is it possible that photons affect spins? The optical electric dipole transition cannot change the spin magnetic quantum number. In addition, because of the quenching of orbital angular momentum in solids, the diagonal elements of the spin–orbit interaction vanish [52]. This fact clearly shows that the most effective spin-flip occurs during the optical transition,

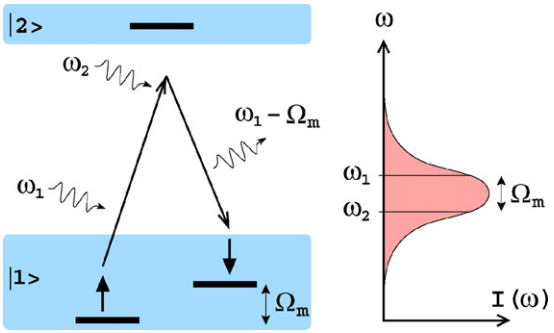

Figure 1. Illustration of the stimulated Raman-like coherent scattering mechanism believed to be responsible for the ultrafast optically generated magnetic field. Two frequency components of electromagnetic radiation from the spectrally broad laser pulse take part in the process. The frequency ω_1 causes a transition into a virtual state with strong spin–orbit coupling. Radiation at the frequency $\omega_2 = \omega_1 - \Omega_m$ stimulates the relaxation back to the ground state with the creation of a magnon with frequency Ω_m.

when the wavefunction of the electron is a superposition of several eigenstates. Note that the spin-flip appears to be far less effective for an electron in one of these stationary states. Similar ideas have been used in theoretical studies of ultrafast laser-induced demagnetization [53] and spin-switching [54]. It was pointed out that even if the spin–orbit interaction in each of the stationary states is small, the cooperative effect of spin–orbit coupling and intense laser radiation may cause efficient spin-flip and lead to ultrafast nonthermal demagnetization of materials. The mechanism that can account for the ultrafast and nonthermal laser control of magnetism can be similar to the process of stimulated Raman scattering (see figure 1).

Let us consider the excitation of spins by a 100 fs laser pulse. Initially the electron is in the ground state $|1\rangle$ and its spin is up. If the state is nondegenerate, being an orbital singlet, the spin–orbit coupling for the electron in this state can be neglected. If we act on this electron with a photon, during the optical transition the wavefunction of the electron becomes a superposition of several eigenstates. This will effectively increase the orbital momentum of the electron, leading to an increased spin–orbit coupling and thus resulting in an intensification of the spin-flip process. If the energy of the photon is small compared to the gap between $|1\rangle$ and the nearest state $|2\rangle$, the photon will not excite any real electronic transition, but just result in the spin-flip of the electron in the ground state. In other words, the spin-flip in the ground state is due to the fact that circularly polarized light mixes a fraction of the excited-state wavefunction into the ground state and causes the perturbed ground state to have a net magnetic moment [24]. The process will be accompanied by the coherent re-emission of a photon of energy $\hbar\omega_2 = \hbar(\omega_1 - \Omega_m)$. In magnetically ordered materials $\hbar\Omega_m$ corresponds to the energy of a magnon. Moreover, such a laser-induced spin-flip process can be coherently stimulated if both frequencies ω_1 and ω_2 are present in the laser pulse (see figure 1). The time of the spin-flip process τ_{sf} is given by the energy of the spin–orbit interaction in the perturbed ground state E_{SO}. For materials with a large magneto-optical susceptibility the energy of the spin–orbit coupling may exceed 20 meV [55] and thus the spin-flip process can be as fast as $\tau_{sf} \sim \hbar/E_{SO} \sim 20$ fs.

Note that such a spin-flip process is allowed in the electric-dipole approximation [52]. In contrast to magnetic dipole transitions probed in magnetic resonance, this mechanism is much more effective and does not require annihilation of a photon. It means that the energy transfer from photons to spins (magnons) is realized via an inelastic scattering process. While some photons lose a small part of their energy, the total number of photons remains unchanged.

It is remarkable that in a spin-flip via stimulated Raman scattering, as described above, the stimulating and re-emitted photons have identical polarizations, implying that such a light-induced spin-flip is not accompanied by a loss of the angular momentum of the photons.

2.2. Experimental studies of the inverse Faraday effect

2.2.1. Inverse Faraday effect in orthoferrites. The rare-earth orthoferrites $RFeO_3$ are a well studied family of magnetic compounds [56]. These materials crystallize in an orthorhombic perovskite-type structure with four molecular units per unit cell, with space-group symmetry ($Pbnm$). The spins of the Fe^{3+} ions ($3d^5$, ground state $^6A_{1g}$, $S = 5/2$) are coupled antiferromagnetically by isotropic exchange. The Dzyaloshinskii–Moriya interaction [57, 58] leads to a slight canting of opposite spins over an angle of about 0.5°, giving rise to a spontaneous magnetization $4\pi M_s = 100$ G at room temperature.

Despite the fact that the magnetization in orthoferrites is small, these materials exhibit a large Faraday rotation owing to their strong spin–orbit interaction [49, 55]. Thus nonthermal effects of light on the spontaneous magnetization are expected to be large in these compounds. Moreover, optical absorption of orthoferrites in the infrared spectral region is low compared to metals (below 200 cm^{-1}) [59], so that thermal effects of light on the magnetization are suppressed significantly.

Optically induced excitation of antiferromagnetic resonance in $DyFeO_3$ using circularly polarized pump pulses was recently demonstrated in [60]. Time-resolved measurements of spin dynamics, performed in this study, were based on a pump-and-probe method and employed amplified subpicosecond pulses from a Ti:sapphire laser. In this method, a laser pulse is split into two parts. The most intensive pulse is used as a pump, while the less intensive one is used as a probe. Both pulses follow different optical paths and are focused to the same spot on the sample. Using the direct magneto-optical Faraday effect, the probe detects the pump-induced changes induced by the pump. Varying the time delay between pump and probe pulses one can monitor the magnetic state of a medium with a temporal resolution limited by the pulse width [61].

Figure 2 shows the temporal behaviour of the Faraday rotation in a $DyFeO_3$ sample cut perpendicular to the [001] crystallographic axis for two circularly polarized pump pulses of opposite helicities. At zero time delay instantaneous changes of the Faraday rotation are observed. These ultrafast changes of the magneto-optical signal can be explained in terms of nonlinear optical polarizations induced during virtual and real optical transitions in the Fe^{3+} ions. The instantaneous changes of the Faraday rotation are followed by oscillations with a frequency of about 300 GHz. Note that the frequency of the oscillations is in excellent agreement with the frequency of antiferromagnetic resonance in $DyFeO_3$. Thus the oscillations of the Faraday rotation can be clearly assigned to spin oscillations. It is seen from the figure that the phase of the laser-triggered spin oscillations depends on the helicity of the pump. Right-handed and left-handed circularly polarized pulses excite spin oscillations of opposite phase. Therefore, this experiment clearly demonstrates the feasibility of the inverse Faraday effect and indicates an ultrafast and efficient coupling between angular momentum of photons and spins.

In order to separate thermal and nonthermal mechanisms of the optical excitation of antiferromagnetic oscillations, one should realize that thermal effects are insensitive to the helicity of the pump light, while the nonthermal excitation with right- σ^+ and left-handed σ^- circularly polarized laser pulses trigger spin waves of opposite phase. Figure 3 shows the difference between the Faraday rotations induced by right- and left-handed circularly polarized pump light in $DyFeO_3(001)$ for the temperature range between 20 and 175 K. It is seen that an increase of the temperature results in an increase of the frequency of the nonthermally induced

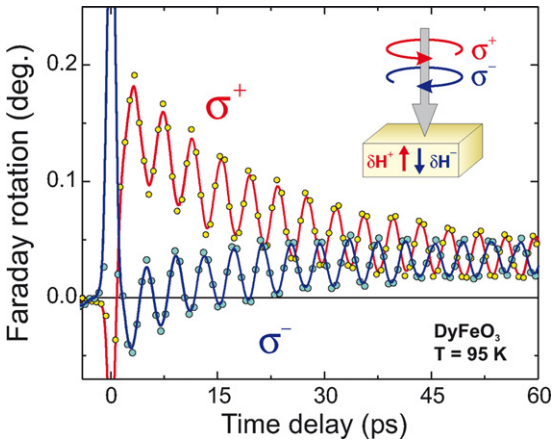

Figure 2. Magnetic excitations in $DyFeO_3$ probed by the magneto-optical Faraday effect. Two processes can be distinguished: (1) instantaneous changes of the Faraday effect due to the photoexcitation of Fe ions and relaxation back to the high-spin ground state $S = 5/2$; (2) oscillations of the Fe spins around their equilibrium direction with an approximately 5 ps period. The circularly polarized pumps of opposite helicities excite oscillations of opposite phase. The inset shows the geometry of the experiment. Vectors δH^+ and δH^- represent the effective magnetic fields induced by right-handed σ^+ and left-handed σ^+ circularly polarized pumps, respectively [60].

oscillations up to 450 GHz at 175 K, while the amplitude of the oscillation decreases. The increase of the frequency of spin oscillations upon temperature increase agrees with results of earlier Raman experiments in $DyFeO_3$ [56, 62, 63] and originates from the temperature dependence of the constants of magnetic anisotropy. Although the decrease of the amplitude of the spin oscillations upon temperature increase has also been seen in Raman scattering experiments [63], we are not aware of an interpretation of such temperature dependence.

The highest value of the amplitude of the nonthermally induced oscillations is observed between 20 and 50 K. The amplitude of the oscillations corresponds to a magnetization change $\Delta M \sim 0.06 \times M_s$, where M_s is the saturation magnetization. This ratio is obtained from hysteresis measurements in a static magnetic field, that shows that the saturated Faraday rotation in a single-domain sample is equal to 1°. A simple estimate shows that spin oscillations with such amplitude can be triggered if a 100 fs laser pulse acts on the spins as an equally short pulse of an effective magnetic field up to 1 T.

The equivalence between a circularly polarized laser pulse and an effective magnetic field can also be seen in the experiments with $DyFeO_3$ samples of different orientations. Figure 4 shows the temperature dependence of the frequencies of the spin oscillations excited by circularly polarized laser pulses. In particular, filled and open circles show the frequencies of the oscillations excited by laser pulses propagating along the [001] and [100] crystallographic axes, respectively. The lines show the temperature behaviour of the frequencies of the quasi-antiferromagnetic and quasi-ferromagnetic modes of magnetic resonance in $DyFeO_3$. The figure clearly shows that laser pulses propagating along the [001] crystallographic axes trigger the quasi-antiferromagnetic mode of the magnetic resonance. Note that this mode can only be triggered if light acts on the spins as an effective magnetic field directed along the [001] axis. Similarly, laser pulses propagating along [100] crystallographic axes trigger the quasi-ferromagnetic mode of the magnetic resonance and this means that a laser pulse acts on the spins as an effective magnetic field directed along the [100] axis. Recently, a detailed

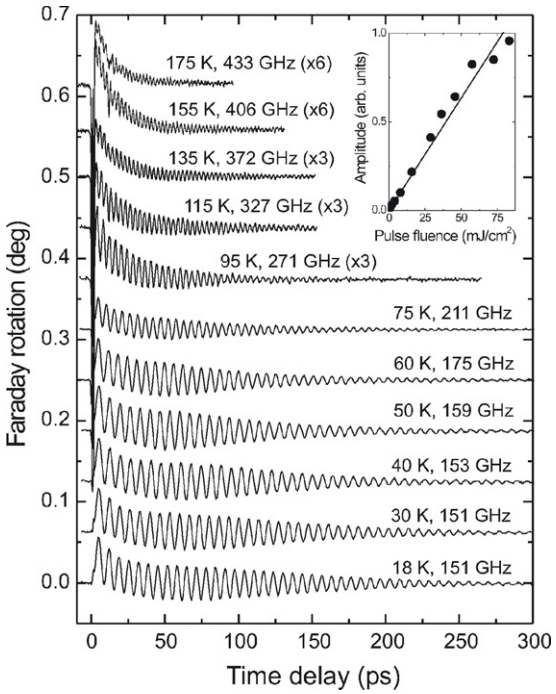

Figure 3. Excitation of the spin oscillations in $DyFeO_3$ measured at different temperatures in the range between 20 and 170 K. In order to exclude effects not relevant to magnetic excitations, the difference between the signals for right- and left-handed circularly polarized pump pulses is plotted. Every new curve is shifted from the previous one along the vertical axis over 0.06°. The inset shows the amplitude of the spin oscillations as a function of pump fluence [60].

investigation of the laser-induced antiferromagnetic resonance has been performed for another rare-earth orthoferrite $TmFeO_3$ [64]. All these studies unambiguously show that a circularly polarized laser pulse acts on the spins as an equally short pulse of an effective magnetic field directed along the wavevector of light.

It must be noted that figure 4 shows that below 50 K the frequencies of the laser-induced spin precession are in disagreement with those obtained earlier in the experiments on infrared absorption and Raman scattering [56, 63]. Recently, the laser-induced spin dynamics in $DyFeO_3$ has been investigated theoretically [65]. The study was based on a solution of the nonlinear Landau–Lifshitz–Gilbert equations for two magnetic sublattices, taking into account their antiferromagnetic coupling and the Dzyaloshinskii–Moriya interaction. In general, the simulations are in excellent agreement with the experiment. Nevertheless, a careful analysis also shows that the frequencies of antiferromagnetic precession observed in the experiment in the range below 50 K are in disagreement with those predicted by the theory. This discrepancy raises a number of intriguing questions about the stability of the magnetic structure of $DyFeO_3$ under laser excitation below 50 K and the feasibility of a nonthermal laser-induced phase transition[3].

In addition to oscillations, figures 2 and 3 also show an exponential decay on a timescale of about 100 ps. One may try to explain this by a laser-induced change of the equilibrium

[3] Recently we have experimentally demonstrated the feasibility of a nonthermal laser-induced magnetic phase transition in $HoFeO_3$ [66].

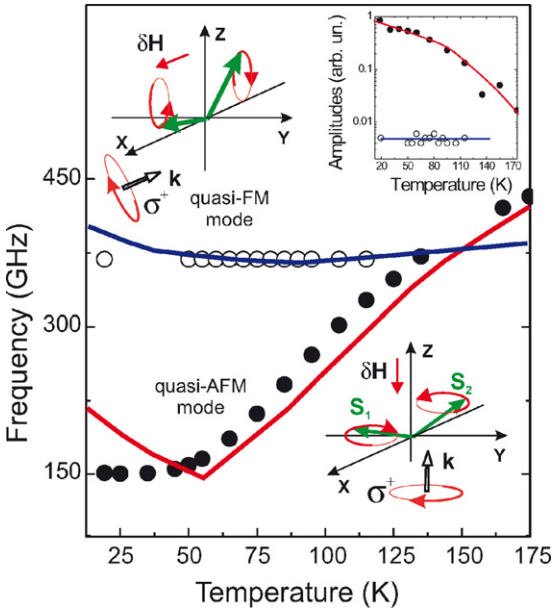

Figure 4. Temperature dependence of the frequencies of the observed spin oscillations. Filled and open circles show the frequencies of the excited oscillations for laser pulses propagating along [001] and [100] crystallographic axes, respectively. Black (red and blue) lines show the frequency of the quasi-antiferromagnetic (quasi-AFM) and the quasi-ferromagnetic (quasi-FM) resonance modes from [56, 63]. The top right inset shows the temperature dependence of the oscillation amplitudes. Top left and bottom right insets are respectively schematic representations of the quasi-FM and quasi-AFM modes of the spin resonance. Vectors δH show the directions of the instantaneous magnetic field that is equivalent to the laser excitation [60].

orientation of the magnetization and subsequent decay of the equilibrium orientation to the initial state. In principle, the effective magnetic field induced via the inverse Faraday effect can cause such a change of the equilibrium orientation. However, according to [65], such a shift of the equilibrium must be negligible in this experiment, because the amplitude of the effective magnetic field is much smaller than the antisymmetrical exchange field. The change of the equilibrium orientation could also be caused by photo-magnetic effects of laser-induced magnetic anisotropy discussed in section 3. However, this interpretation has not found an experimental confirmation up to now. Therefore, the origin of the exponential decay of the equilibrium level on a timescale of about 100 ps is still an open question.

2.2.2. Inverse Faraday effect in garnets. For about 50 years magnetic garnets have been one of the most popular types of magnetic dielectric materials for both research and applications [67, 68]. Their physical properties are well known and can be tailored over a wide range through chemical substitution and by varying their growth conditions. For decades they have been considered ideal model systems for the experimental and theoretical investigation of magnetic phenomena. These materials are ferrimagnets and the linewidth of ferrimagnetic resonance in garnets can be extremely narrow, implying a very low damping of magnetic excitations [67]. For these reasons they seem to be good candidates for the study of ultrafast spin dynamics in general and the search for nonthermal mechanisms for the optical control of magnetization in particular [48, 69, 70].

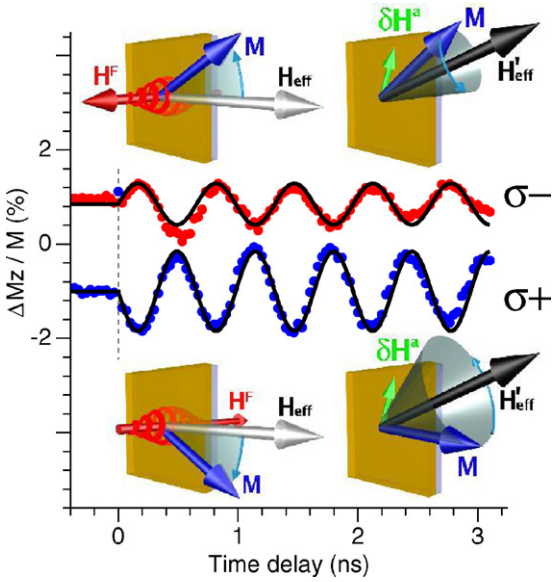

Figure 5. Precession following excitation with circularly polarized light. The two helicities σ^+ and σ^- give rise to precession with opposite phases and different amplitudes. During the 100 fs presence of the laser pulse the magnetization precesses in the dominating axial magnetic field $\mathbf{H}_\mathrm{F}$ created by the circularly pump pulse. Subsequent precession takes place in the effective magnetic field $\mathbf{H}'_\mathrm{eff} = \mathbf{H}_\mathrm{eff} + \delta\mathbf{H}^\mathrm{a}$ [69, 70]. $\delta\mathbf{H}^\mathrm{a}$ represents photo-induced magnetic anisotropy discussed in section 3.

Optically induced ferrimagnetic resonance in magnetic garnets using circularly polarized pump pulses was recently demonstrated in [69, 70]. In particular, right and left circularly polarized laser pulses were used to excite magnetic garnet films of the composition $Lu_{1.69}Y_{0.65}Bi_{0.66}Fe_{3.85}Ga_{1.15}O_{12}$. The films were grown on (001) oriented gallium gadolinium garnet (GGG) substrates by liquid phase epitaxy. Small amounts of Pb impurities are known to exist in these types of films due to the flux from which they are grown. Applying an external magnetic field $\mathbf{H}_\mathrm{ext}$ in the plane of a magnetic garnet sample and pumping with circularly polarized laser pulses, precession of $\mathbf{M}$ with opposite phase and different amplitude was triggered by pulses of helicity σ^+ and σ^-; see figure 5.

Similarly to orthoferrites, these experimental observations can be understood if during the presence of the laser pulse a strong magnetic field along the $\mathbf{k}$ vector of light is created. Such an axial magnetic field $\mathbf{H}^\mathrm{F}$ can be generated by intense circularly polarized light through the inverse Faraday effect [23–25, 60]. In this experiment the optically generated field pulses are much stronger than both anisotropy $\mathbf{H}_\mathrm{a}$ and the applied field $\mathbf{H}_\mathrm{ext}$ and therefore completely dominate during the $\Delta t = 100$ fs presence of the laser pulse. The magnetization will respond by precessing in the plane of the film (normal to $\mathbf{H}^\mathrm{F}$) to a new in-plane orientation. After the pulse is gone, the magnetization will precess in the effective in-plane field $\mathbf{H}'_\mathrm{eff} = \mathbf{H}_\mathrm{ext} + \mathbf{H}_\mathrm{a}$, as illustrated in figure 5. The strength of the photo-induced field $\mathbf{H}^\mathrm{F}$ can be estimated from the precession amplitude Λ:

$$H^\mathrm{F} \approx \frac{\omega}{\gamma} \approx \frac{\Lambda}{\gamma\,\Delta t_\mathrm{pulse}} \tag{3}$$

where ω is the precession frequency, γ is the gyromagnetic ratio and Δt_pulse is the duration of

the optical pulse. We find that laser pulses of energy 20 μJ focused to a spot of about 10^{-4} cm^2 create transient magnetic field pulses of about 0.6 T in the garnet films.

An important conclusion can be drawn from the experimental results present in figure 5. It can be seen that during the action of the laser pulse the magnetization remains in the plane of the sample, keeping the z-component of magnetization unchanged. Therefore the laser control of magnetization is not accompanied by direct angular momentum transfer from photons to spins.

In conclusion of this section we would like to note that the main requirement for a large opto-magnetic effect is a large magneto-optical susceptibility. Thus we are strongly convinced that materials that exhibit opto-magnetic phenomena are not limited to orthoferrites and garnets only. Opto-magnetism must also be present in other materials possessing strong magneto-optical effects.

3. Laser control of magnetic anisotropy and ultrafast photomagnetism

3.1. The phenomenon of photo-induced magnetic anisotropy

Photomagnetic effects differ from the opto-magnetic ones by that the former are related to the absorption of the light [47]. Simple estimates show that, at the light intensities met in experiments, absorption can hardly result in an effective change of the magnetization. Nevertheless, an absorption of laser radiation may result in a change of magnetic anisotropy of a compound. Effects of photo-induced magnetic anisotropy are known to exist in magnetic dielectrics [47, 48]. The most common condition for these effects is the presence of highly anisotropic photosensitive ions in a crystal lattice, such as Fe^{2+} in Si-doped or Co^{2+} in Co-doped iron garnets [71, 72]. For instance, in Co-doped iron garnets Co^{2+} and Co^{3+} ions occupy octahedral cites of the crystal cell. An octahedral Co^{3+} ion gives zero contribution to the total magnetic anisotropy in a single-ion approximation, while the contribution of octahedral Co^{2+} is very large, being three orders of magnitude larger than that of Fe^{3+}. An optical excitation of Co-doped garnets can result in a spatial redistribution of the highly anisotropic Co^{2+} ions and can thus lead to modification of the magnetic anisotropy [73–76]. Normally, the effect of the photo-induced magnetic anisotropy gets larger at lower temperatures. Nevertheless, even at room temperature this photomagnetic effect can be strong and result in reconstruction of domain patterns. Figure 6 shows an image of magnetic domains in a garnet film at room temperature and the reconstruction of these domains under the influence of linearly polarized optical excitation. Note that the photo-induced anisotropy in garnet films is strongly dependent on the polarization of light, so that optical excitation with two different polarizations result in different domain patterns. It should be mentioned that the effect of photo-induced magnetic anisotropy has also been observed in undoped garnet samples containing Pb impurities [77].

3.2. Time-resolved studies of the photo-induced magnetic anisotropy

Recently time-resolved studies of the photo-induced magnetic anisotropy have been performed with subpicosecond resolution. Applying an external magnetic field $\mathbf{H}_{\text{ext}}$ in the plane of a magnetic garnet sample (so that $\mathbf{M}$ is in plane, $\zeta = 90°$) and pumping with linearly polarized laser pulses (see figure 7), optically triggered precession of the magnetization $\mathbf{M}$ was observed; see figure 8(a). Intriguingly, the amplitude and phase of the precession in figure 8(a) was found to depend on the plane of polarization θ of the pump pulses as shown in figure 8(b). Negative values of the amplitude indicate precession of $\mathbf{M}$ with opposite phase. Extrema of the precessional amplitude (of opposite phase) were observed for every 90° rotation of the

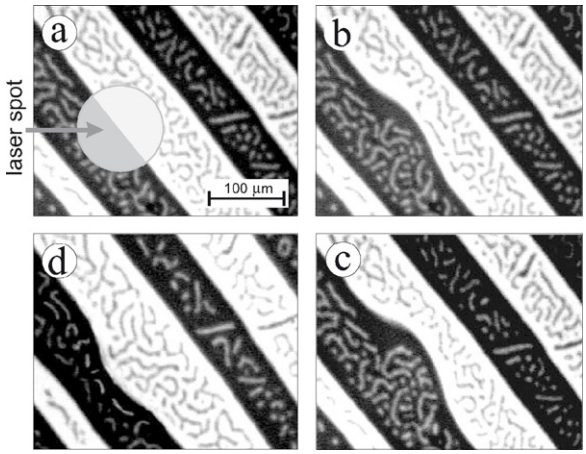

Figure 6. Images of magnetic domains in a $Y_2CaFe_{3.9}Co_{0.1}GeO_{12}$ film at room temperature: (a) the image before illumination; (b), (d) the domain patterns after illumination with linearly polarized light, with polarization along $[1\bar{1}0]$ and [110] crystallographic axes, respectively; (c) the domain pattern after illumination with light polarized along [110] in an external magnetic field of 10 Oe along the [110] direction [74].

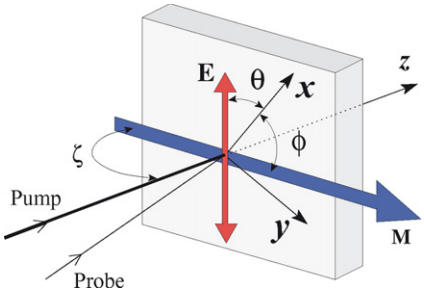

Figure 7. Experimental geometry of photoexcitation of magnetic garnet films by polarized laser light. Pump and probe pulses were incident on the garnet film at near normal incidence. The magnetization **M** of the sample forms an angle ζ with the sample normal [001] and an angle ϕ with the crystallographic [100] x-axis of the film. For linearly polarized pump pulses the angle of the electric field component of light **E** with respect to the sample x-axis is denoted θ.

polarization, and at some polarizations no precessional dynamics was triggered. From this dependence on pump polarization it is evident that the underlying effect must be nonthermal. An ultrafast heating effect would only reduce the magnitude of the magnetization and the anisotropy field independently of the pump polarization. Heating effects thus cannot be responsible for triggering magnetization dynamics that exhibit polarization dependence of the type that we observe in figure 8.

It is also interesting to note that **M** always starts its precessional motion by moving normal to the film plane along the $\pm\hat{z}$-direction. This follows from the initial phase of the measured signal in figure 8(a), which always starts from the inflection point where M_z is changing most rapidly. From the Landau–Lifshitz equation it can be inferred that immediately after the photoexcitation both **M** and $\mathbf{H}_{\text{eff}}$ are in the film plane but not parallel to each other. Consequently, the observed magnetization dynamics must be due to an ultrafast change of the magnetization $\delta\mathbf{M}$,

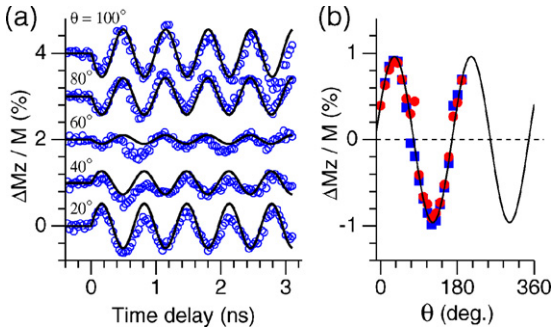

Figure 8. Coherent precession of the magnetization triggered by linearly polarized laser pulses. (a) Time dependence of the precession for different planes of pump polarization θ, with an applied field of $|\mathbf{H}_{\text{ext}}| = 350$ Oe in the plane of the sample. Circles represent measurements and solid lines simulations based on the Landau–Lifshitz equation. (b) Precessional amplitude as a function of the plane of pump polarization. Round (red) and square (blue) symbols represent amplitudes extracted from measurements at $\pm\mathbf{H}_{\text{ext}}$. The solid line is a best fit [70].

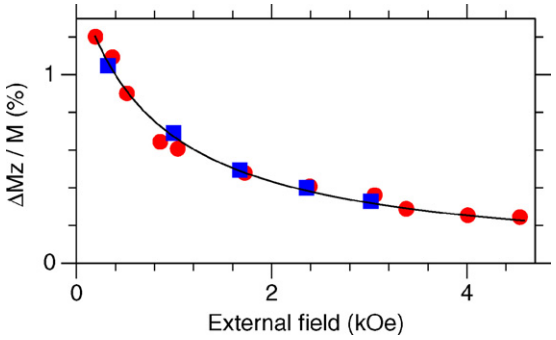

Figure 9. Dependence of the precessional amplitude on the applied in-plane magnetic field $\mathbf{H}_{\text{ext}}$. Round and square symbols represent amplitudes extracted from measurements at $\pm\mathbf{H}_{\text{ext}}$.

the anisotropy field $\delta\mathbf{H}^{\text{a}}$, or a combination of the two, that effectively creates an in-plane angular displacement $\Lambda = \angle(\mathbf{M}, \mathbf{H}_{\text{eff}})$ between $\mathbf{M}$ and $\mathbf{H}_{\text{eff}}$. It is possible to distinguish between these possibilities by analysing the precession amplitude Λ as function of the applied field. The result is shown in figure 9. If triggered by an ultrafast rotation of the magnetization $\mathbf{M} \rightarrow \mathbf{M} + \delta\mathbf{M}$, the amplitude Λ of the subsequent precession should be independent of the strength of the applied magnetic field as $\angle(\mathbf{M}, \mathbf{H}_{\text{eff}})$ does not depend on $\mathbf{H}_{\text{ext}}$. However, if the precession is caused by a change in the effective field through a photoinduced anisotropy field $\delta\mathbf{H}^{\text{a}}$, the precession amplitude Λ is expected to decrease with increasing applied magnetic field as

$$\Lambda = \angle(\mathbf{H}_{\text{eff}}, \mathbf{H}_{\text{eff}} + \delta\mathbf{H}^{\text{a}}) \propto \frac{1}{|\mathbf{H}_{\text{ext}} + \mathbf{H}_{\text{a}}|} \tag{4}$$

which is valid for small amplitude precessions. As shown by the fitted curve in figure 9 (solid line), the measurements exhibit the exact behaviour that one expects for a photoinduced anisotropy field $\delta\mathbf{H}^{\text{a}}$ (equation (4)). Based on the precession amplitude, the magnitude of the photoinduced field can be estimated to be $\delta H^{\text{a}} = 0.5$ Oe for the present geometry ($\zeta = 90°$). A graphical illustration of the excitation process and the subsequent precession is shown in figure 10.

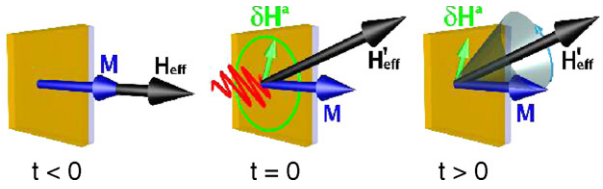

Figure 10. Graphical illustration of the process of photoinduced magnetic anisotropy caused by linearly polarized laser excitation and the subsequent precessional dynamics.

The creation of a static magnetic field $\delta\mathbf{H}^{\mathrm{a}}(0)$ in the sample can be described using a simple phenomenological equation:

$$\delta H_i^a(0) = \chi_{ijkl} E_j(\omega) E_k(\omega) M_l(0). \tag{5}$$

Here E is the electric field component of light and M is the magnetization of the garnet film. The fourth-rank polar tensor χ_{ijkl} has nonzero components for crystals of any symmetry [78].

When taking the experimental geometry (figure 7) and the symmetry of χ_{ijkl} for the 4 mm point group of our samples into account, only four independent nonzero components of the tensor χ_{ijkl} remain,

$$\begin{aligned} A &= \chi_{xxxx} = \chi_{yyyy} \\ B &= \chi_{xyxy} = \chi_{xxyy} = \chi_{yxyx} = \chi_{yyxx} \\ C &= \chi_{xyyx} = \chi_{yxxy} \\ D &= \chi_{zxxz} = \chi_{zyyz} \end{aligned}$$

and the vector components of the photoinduced anisotropy field are then given by

$$\delta H_x^a \propto E_0^2 M_{\mathrm{s}} \sin\zeta[(A+C)\cos\phi + (A-C)\cos 2\theta\cos\phi + 2B\sin 2\theta\sin\phi] \tag{6}$$

$$\delta H_y^a \propto E_0^2 M_{\mathrm{s}} \sin\zeta[(A+C)\sin\phi - (A-C)\cos 2\theta\sin\phi + 2B\sin 2\theta\cos\phi] \tag{7}$$

$$\delta H_z^a \propto E_0^2 M_{\mathrm{s}} D\cos\zeta. \tag{8}$$

Here δH_i^a is the photoinduced field along the i-direction, $i = \{x, y, z\}$ refers to the crystal axes of the sample, ϕ denotes the azimuthal angle between the sample x-axis and the projection of the magnetization vector on the film plane and ζ is the angle between the film normal and the magnetization, as shown in figure 7.

From these equations one can see that if the magnetization $\mathbf{M}$ is in the film plane, the out-of-plane component δH_z of the photoinduced anisotropy field does not contribute as $\cos\zeta = 0$. This is in accordance with our experimental results from figure 8, which show an in-plane $\delta\mathbf{H}^{\mathrm{a}}$. However, in order for the above equations to describe a field $\delta\mathbf{H}^{\mathrm{a}}$ consistent with the polarization dependence of the precession amplitude, shown in figure 8(b), the number of independent tensor components must be further reduced. The fact that there is no amplitude offset in the curve shown in figure 8(b) requires that $A = -C$, so that the first term in equations (6) and (7) vanishes. Furthermore, the sinusoidal shape of the curve implies that $A = B$ and leaves us with only two independent components of the tensor χ_{ijkl},

$$\begin{aligned} A &= \chi_{xxxx} = \chi_{yyyy} = -\chi_{xyyx} = -\chi_{yxxy} \\ &= \chi_{xyxy} = \chi_{xxyy} = \chi_{yxyx} = \chi_{yyxx} \\ D &= \chi_{zxxz} = \chi_{zyyz}. \end{aligned}$$

These additional equalities indicate that the χ_{ijkl} tensor has a higher symmetry than the garnet crystal. Note that this does not violate Neumann's principle, which states that the symmetry

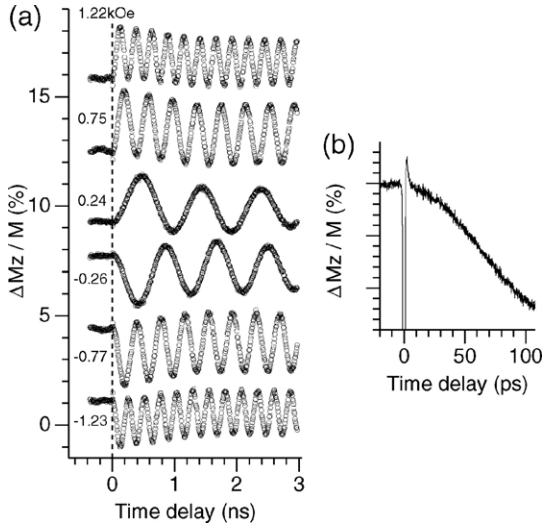

Figure 11. (a) Precession of the magnetization following excitation with linearly polarized light for different values of the magnetic field applied at an angle of about 45° with the sample normal. (b) The excitation shown on a finer timescale [70].

elements of any physical property of a crystal must include all the symmetry elements of the point group of the crystal [78]. This does not prevent that property from having a higher symmetry than the crystal. The optically induced anisotropy field can now be written as

$$\delta H_x^a \propto A E_0^2 M_s \sin\zeta\,[\sin 2\theta \sin\phi + \cos 2\theta \cos\phi] \tag{9}$$

$$\delta H_y^a \propto A E_0^2 M_s \sin\zeta\,[\sin 2\theta \cos\phi - \cos 2\theta \sin\phi] \tag{10}$$

$$\delta H_z^a \propto D E_0^2 M_s \cos\zeta. \tag{11}$$

For the in-plane field geometry ($\cos\zeta = 0$) this describes a vector of constant length and with a direction depending on the angle ϕ of the magnetization with respect to the x-axis and the plane of polarization θ of the pump pulses. Computer simulations based on this simple model and the numerical integration of the Landau–Lifshitz equations exhibit good agreement with our experimental results for the in-plane $\mathbf{H}_{\text{ext}}$ geometry shown in figure 8(a). However, although such a phenomenological model may describe the symmetry properties of the phenomenon observed, it does not provide any insight into the microscopic mechanism responsible for the laser-induced magnetic field $\delta\mathbf{H}^a$. Equation (5) can describe both the photomagnetic effect of laser-induced magnetic anisotropy and the opto-magnetic inverse Cotton–Mouton effect (ICME)[4]. Note that the opto-magnetic ICME, similarly to the inverse Faraday effect, is present only during the action of the laser pulse, while the photo-induced magnetic anisotropy is expected to remain longer after the laser excitation.

In order to estimate the lifetime of the laser-induced magnetic field $\delta\mathbf{H}^a$, an experiment in an external field at an angle with respect to the film plane was performed. In this case the magnetization can be tilted out of the film plane ($\zeta < 90°$) and $\delta H_z \neq 0$. The actual angle ζ that the magnetization makes with the film normal is determined by the balance between the applied field, the anisotropy field and the demagnetizing field. When pumping with linearly polarized laser pulses in this configuration, a larger amplitude precession was observed; see figure 11(a). This precession is superimposed on a slowly decaying exponential background

[4] Recently an ultrafast opto-magnetic inverse Cotton–Mouton effect was observed in $FeBO_3$ [79].

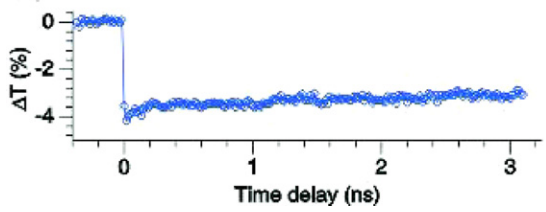

Figure 12. Pump-induced change of the sample transmittivity ΔT [70].

caused by the relaxation of the photoinduced anisotropy. In contrast to the in-plane applied field geometry (where $\zeta = 90$), the initial phase of the precession in figure 11(a) reveals that for **M** tilted out of the film plane ($\zeta < 90°$) the initial motion of **M** is nearly parallel to the film plane. This implies that the laser-induced $\delta\mathbf{H}^{\mathrm{a}}$ is directed essentially along the z-direction. The dependence of the precession amplitude and phase on the polarization of the pump pulses becomes gradually smaller as **M** is tilted further out of the film plane. At about $\zeta = 60°$, all polarization dependence is practically gone and changing the polarity of the external field gives a near 180° phase shift in the measured signal. From the precession amplitude in figure 11 the strength of the photoinduced anisotropy field is estimated to be $\delta H^{\mathrm{a}} = 1.5$ Oe.

Laser heating effects in the sample, if present, are likely to be more pronounced in this geometry than in the in-plane field geometry, as a thermal reduction of **M** also changes the equilibrium $\mathbf{H}_{\mathrm{eff}}$ and leads to a reorientation of **M** along the z direction. However, in our experiments the optical excitation of coherent spin waves is ultrafast (see figure 11 (b), where very fast initial relaxation of less than a few picoseconds is indicated), much faster than the phonon–magnon interaction time, which is about 1 ns in this material [67]. The optical excitations of spin waves therefore cannot be of thermal origin. As was discussed in [70], thermal effects can be seen on the timescale of a few nanoseconds when the sample is heated to temperatures near the Curie point.

Based on the results in figure 11(a), one can argue that the lifetime τ of $\delta\mathbf{H}^{\mathrm{a}}$ is longer than the time $t_{\mathrm{exp}} = 3$ ns accessible in this experiment. As the precession of **M** is always around the effective magnetic field $\mathbf{H}'_{\mathrm{eff}} = \mathbf{H}_{\mathrm{eff}} + \delta\mathbf{H}^{\mathrm{a}}$, any relaxation of $\delta\mathbf{H}^{\mathrm{a}}$ should be visible in the time trace of the precession. Note in figure 11(a) how **M** precesses around an equilibrium $\mathbf{H}'_{\mathrm{eff}}$ that is different from the initial $t < 0$ state. Some relaxation of $\mathbf{H}'_{\mathrm{eff}}$ can be seen (the slow overall change of the fast oscillating signal), but this is not sufficient to restore the original equilibrium on the timescale of the experiment. This indicates that after $t_{\mathrm{exp}} = 3$ ns $\delta\mathbf{H}^{\mathrm{a}}$ has still not decayed completely. Thus, one can conclude that $\delta\mathbf{H}^{\mathrm{a}}$ is due to the photomagnetic effect of the laser-induced magnetic anisotropy and not due to the opto-magnetic ICME. Note that the photoinduced change in the sample transmittivity ΔT shown in figure 12 also does not relax significantly during 3 ns.

There appears to be a linear relation between the precession amplitude and the pump power up to pulse energies of almost 10 μJ (figure 13(b)). At higher pulse energies the effect saturates completely. Based on the absorption coefficient the estimated density of absorbed photons is about one per hundred unit cells in the illuminated crystal volume. The saturation of $\delta\mathbf{H}^{\mathrm{a}}$ at high pump intensities may be attributed to the Pb impurities. The low concentration of Pb impurities creates a limited number of photoactive ions and the photomagnetic effect can therefore be expected to saturate under intense illumination. An estimate for our sample shows that the illuminated volume of garnet film contains about 10^{12} Pb ions. An optical pulse of 20 μJ delivers 10^{14} photons, from which about 1% are expected to be absorbed. This allows, in principle, for all of the photoactive ions to be excited, and it is thus not surprising that saturation

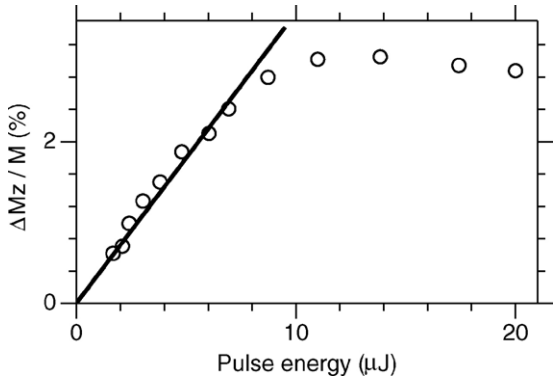

Figure 13. Dependence of precession amplitude on the excitation pulse energy [70].

can occur at these pump intensities. This saturation of the precession amplitude at relatively low power also supports the conclusion that $\delta\mathbf{H}^{a}$ is due to the photomagnetic effect of the laser-induced magnetic anisotropy. Note that the ICME is expected to behave similarly to the inverse Faraday effect, which did not saturate in the studied range of intensities.

Another time-resolved magneto-optical study of the laser-induced modification of magnetic anisotropy has been performed for the antiferromagnetic dielectric NiO [80, 81]. As the magnetic anisotropy is determined by dipolar and quadrupolar interactions between the magnetic moments, it is easily modified by the shift of 3d orbital wavefunctions accompanying the excitation of d–d transitions by a pump pulse. This may lead to a change of the easy direction of the single-ion magnetic anisotropy from $[11\bar{2}]$ to [111]. Duong *et al* probed the magnetic changes following the photo-excitation of NiO by optical second-harmonic generation [80]. The measurements revealed oscillations of the nonlinear optical signal with two frequencies of about 54 and 108 GHz (see figure 14). It is remarkable that, in contrast to the experiments in magnetic garnets, these frequencies do not correspond to those of magnetic resonance but to the magnetic anisotropy energy of 0.11 meV instead. The observed oscillations of the second harmonic are explained by quantum beating, which arises from the fact that the $[11\bar{2}]$ ground state and the [111] excited state interfere coherently.

In conclusion of this section we would like to note that there are no fundamental obstacles that prevent the existence of photomagnetic effects of laser-induced magnetic anisotropy in metals and semiconductors. In fact, nonthermal effects of the laser-induced magnetic anisotropy have been recently observed in the III–V ferromagnetic semiconductor (Ga, Mn)As [43]. The microscopic mechanism of this phenomenon in this novel semiconductor remains an intriguing issue.

4. Coherent control of magnetic precession

4.1. Double-pump coherent magnetization control via the inverse Faraday effect

Ultrafast coherent control of the spin precession can be achieved by using multiple laser pulses in rapid succession.

In figure 15 it is shown how a pump pulse of helicity σ^{+} arriving at $t = 0$ triggers precession of the magnetization, as explained in the previous section. A second pump pulse of helicity σ^{-} arriving after an odd number of half precessional periods rotates the magnetization further away from $\mathbf{H}_{\mathrm{eff}}$, causing the subsequent precession to have almost twice the amplitude.

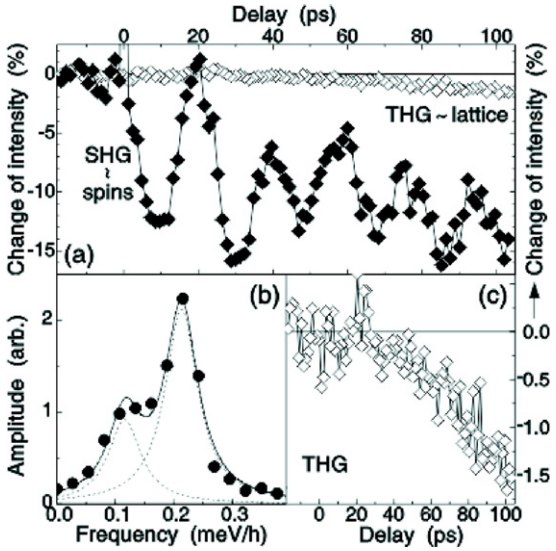

Figure 14. Temporal behaviour of second-harmonic generation (SHG) and third-harmonic generation (THz) measured in reflection from an NiO(111) single crystal at 6 K. (b) Fourier transform of the SHG data after subtraction of the steplike decrease at $t = 0$. Dashed and straight lines: fitted spectral contributions and envelope. (c) THG signal from (a) [80].

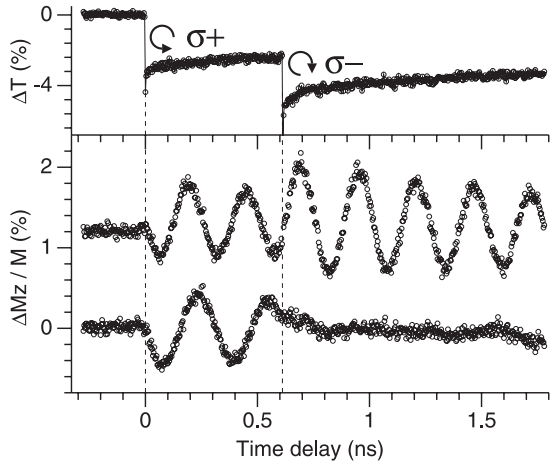

Figure 15. Double-pump experiment in magnetic garnet with circularly polarized laser pulses of opposite helicity and 15 μJ pulse power. The upper panel shows the pump-induced change of the sample transmittivity due to the photoexcitation of impurities. The lower panel shows how amplification and complete stopping of the magnetization precession can be achieved depending on the phase of the precession when the second laser pulse arrives. The time delay between the two pump pulses is fixed at approximately 0.6 ns, and the precession frequency is controlled by varying the external field [70].

If, however, this second pump pulse arrives after an integer number of full periods, the magnetization is rotated back into its original equilibrium orientation along $\mathbf{H}_{\text{eff}}$ and no further precession takes place. Figure 16 gives a pictorial illustration of these two situations.

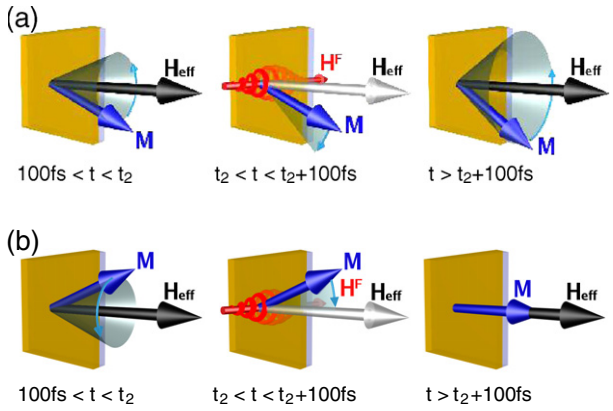

Figure 16. Illustration of the double-pump experiment for circularly polarized pump pulses of opposite helicity arriving at an (a) odd number of half precessional periods and (b) an integer number of full precessional periods. The magnetization is either rotated further away from the effective field direction, causing subsequent precession to take place with almost twice the original amplitude, or the magnetization is rotated back into the effective field direction and no further precession takes place.

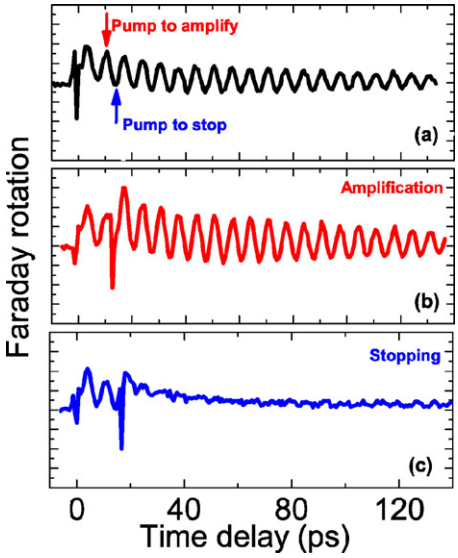

Figure 17. Coherent control of spins in $DyFeO_3$ with two circularly polarized laser pulses: (a) precession triggered by the first laser pulse; (b) amplification of spin precession by the second laser pulse, that comes after an even number of full periods; (c) stopping of the spin oscillations by the second pump, that comes after an odd number of half periods.

Similarly, circularly polarized light can control the precession of antiferromagnetic spins in the THz domain (see figure 17). These experiments clearly demonstrate that femtosecond optical pulses can be used to directly and coherently control spin dynamics. Depending on the phase of the precession when the second pulse arrives, energy is either transferred from the laser pulse to the magnetic system (amplification of the precession) or from the magnetic excitation to the optical pulse (stopping of the precession). In view of the low intrinsic damping in the orthoferrites and garnets, and therefore the long lifetime of magnetic excitations, it is

remarkable how ultrashort laser pulses can completely stop the long-period coherent precession of spins instantaneously. This process of transferring the energy back into the optical pulse can also be viewed as coherent laser cooling of magnons.

The complex spin oscillations in orthoferrites triggered by a train of laser pulses have recently been studied theoretically using nonlinear Landau–Lifshitz–Gilbert equations. It has been demonstrated that such a periodical excitation of spins results in various patterns of spin oscillations, which depend on the intensity and periodicity of the laser pulses [82].

It should be pointed out that the present double-pump experiments, which demonstrate control of the magnetization in ferrimagnetic garnets and antiferromagnetic orthoferrites, are considerably different from those previously reported in diamagnetic and paramagnetic materials. During the past two decades a great number of publications has been devoted to the photoexcitation of a nonequilibrium spin polarization in direct bandgap semiconductors through the phenomena of optical orientation [83–85]. In these materials, absorption of circularly polarized photons may lead to a nonequilibrium population of spin polarized electrons and holes in the conduction band and valence band, respectively. In paramagnetic semiconductors these spin polarized carriers can cause partial alignment of the moments of magnetic ions due to an sp–d exchange interaction, and thereby also affect their precession in a magnetic field [86]. Using this phenomenon of optical orientation, Akimoto *et al* [87] have demonstrated control of the precession of Mn^{2+} moments in $CdTe/Cd_{1-x}Mn_xTe$ quantum wells. Note that this approach, in contrast to our experiments, is based on the absorption of photons. A nonabsorptive mechanism for manipulation of spins in $Zn_{1-x}Cd_xSe$ quantum well structures was reported by Gupta *et al* [88], who used below bandgap optical pulses to control the spin precession of photoexcited electrons in the conduction band via the optical Stark effect. However, these experiments were performed on paramagnetic materials, where coupling between the spins of magnetic ions is small and the spins oscillate independently. Therefore, in a double-pump experiment with paramagnets, the first and second laser pulses can simply excite different spins so that the integrated signal will show either amplification or quenching of the oscillations. Nevertheless, the amplification and quenching of the oscillations in such an experiment would only mean that the spins excited by the first and second pump pulses oscillate in phase or out of phase, respectively. In magnetically ordered materials, discussed in this review, spins are strongly coupled by the exchange interaction and spin excitations are delocalized. Therefore, in contrast to paramagnets, laser control of spins in magnetically ordered materials indeed means control of the collective motion of spins. Additionally, control of the spin precession in paramagnetic semiconductors requires very low temperatures, typically below 10 K, and strong magnetic fields of several tesla. In contrast, the optical control of magnetization reported here can be done at room temperature and in applied static magnetic fields well below 1 kOe.

4.2. Single-pump ultrafast photomagnetic switching

A proper combination of the inverse Faraday effect and the photoinduced anisotropy allows for an interesting demonstration of photomagnetic switching on the femtosecond timescale [69].

In figure 18 the coherent precession of the magnetization following excitation with pulses of helicity σ^- and σ^+ is shown for different values of $\mathbf{H}_{\text{ext}}$. It can be shown (see [69]) that also circularly polarized pump pulses give rise to a change in magnetic anisotropy $\delta\mathbf{H}^{\text{a}}$. The observed precession amplitude is consistently larger in the case of σ^+, as during $0 < t < 100$ fs, $\mathbf{M}$ precesses away from the new equilibrium created by $\delta\mathbf{H}^{\text{a}}$. For pulses of helicity σ^-, this precession is towards the new equilibrium, leading to a smaller precessional amplitude in the time after the pulse (see also figure 5). With an applied field of $|\mathbf{H}_{\text{ext}}| \approx 150$ Oe, no

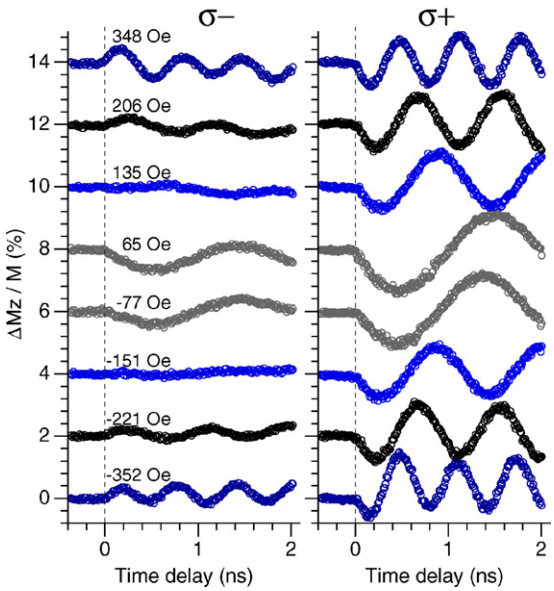

Figure 18. Precession of the magnetization triggered by left- and right-handed circularly polarized laser pulses at different values of the in-plane applied magnetic field. For the σ^- helicity, at an applied field of $\sim \pm 150$ Oe, no precession is observed due to a perfect balance of the two photomagnetic effects $\delta\mathbf{H}^{\mathrm{a}}$ and $\mathbf{H}^{\mathrm{F}}$.

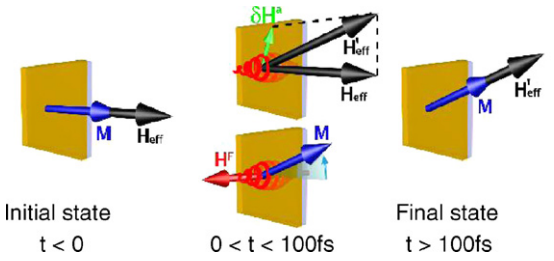

Figure 19. Illustration of the switching process. Initially at $t < 0$ the magnetization is along $\mathbf{H}_{\mathrm{eff}}$. During the presence of the laser pulse $0 < t < 100$ fs photo-induced modification of the anisotropy fields leads to a new long-lived equilibrium along $\mathbf{H}'_{\mathrm{eff}}$. Simultaneously, the strong opto-magnetically generated field $\mathbf{H}^{\mathrm{F}}$ causes the magnetization to precess into the new state. After $t > 100$ fs the optical pulse is gone and the approximately 0.6° switching of $\mathbf{M}$ is complete [70].

precession is triggered due to a perfect balance of two effects: the in-plane precession of the magnetization during the 100 fs magnetic field pulse $\delta\mathbf{H}^{\mathrm{F}}$ brings the magnetization exactly to its new equilibrium orientation created by the optically modified anisotropy field. It remains stable in this orientation until the anisotropy field relaxes back to its original state, i.e. for several nanoseconds. An illustration of this switching process is shown in figure 19.

Note also that for the σ^- helicity at weak applied fields the precession has an opposite phase compared to the precession in stronger applied fields, and that this phase is the same as for the precession triggered by the σ^+ pulses. At weak fields the direction of the photoinduced $\delta\mathbf{H}^{\mathrm{a}}$ is such that the precession of $\mathbf{M}$ in $\mathbf{H}^{\mathrm{F}}$ during the optical pulse is not sufficient to bring it into the direction of $\mathbf{H}'_{\mathrm{eff}}$. At stronger fields, however, $\delta\mathbf{H}^{\mathrm{a}}$ is in a different direction, producing an $\mathbf{H}'_{\mathrm{eff}}$ that is less inclined with respect to the original effective field. During the presence of

$\mathbf{H}^{\mathrm{F}}$ the magnetization now precesses past the direction of $\mathbf{H}'_{\mathrm{eff}}$, and therefore with the opposite phase in the time directly after the laser pulse.

5. Conclusion

This review summarizes recent work on laser control of spins in magnetic dielectrics. It is shown that in contrast to what was accepted earlier, such dynamics can occur at very short timescales. This happens due to strong photo- and opto-magnetic effects. With the help of these effects the strongly coupled spins of magnetically ordered material can directly and coherently be controlled on the femtosecond timescale with ultrashort laser pulses.

Regarding the abovementioned experiments on dielectrics one may expect similar opto-magnetic phenomena in semiconductors in the spectral range below the bandgap. Indeed, recent theoretical work predicts ferromagnetism in undoped diluted magnetic semiconductors illuminated by intense sub-bandgap laser radiation [89]. Microscopically, the mechanism of the photo-induced ferromagnetism is assigned to spin–spin interaction mediated by virtual states.

Regarding metals, we would like to note two things. First of all, we are strongly convinced that laser control of magnetism via the inverse Faraday effect is possible in metals as well[5]. The physics of the inverse Faraday effect in metals in the far-infrared spectral range, where the optical response is determined by free electrons, is expected to be similar to the physics of this phenomenon in a plasma [26, 27, 91]. Second, according to theoretical investigations, the microscopic mechanisms similar to those responsible for the inverse Faraday effect may also result in full, ultrafast and nonthermal demagnetization of metals [53]. Recently, it was argued that the experimental conditions required for ultrafast and nonthermal demagnetization of metals cannot be met experimentally [12]. The argumentation was based on the fact that in a real experiment one typically has about 0.01 photon per site. This small number in combination with the circular dichroism of about 0.01 would yield a direct photon-induced magnetization of at most 10^{-4} μ_{B} per site. Indeed, circular dichroism can hardly account for the laser-induced demagnetization. However, as has been shown above, laser control of magnetism requires neither annihilation of a photon nor loss of its angular momentum. Instead, the mechanism of stimulated Raman scattering using the intrinsic band-width of femtosecond laser pulses may be responsible for the observed strong effects. Therefore, ultrafast and nonthermal laser-induced demagnetization in metals must be feasible.

Finally, we would like to note that, given recent progress in the development of the compact ultrafast lasers [92], the effects discussed in this review provide new prospects for application of opto- and photomagnetic phenomena in magnetic recording and information processing technology.

Acknowledgments

The authors thank Andrzej Maziewski, Andrzej Stupakiewicz, Manfred Fiebig and C A Perroni for useful discussions and illustrations which they supplied for this review. This work was supported by The European RTN network DYNAMICS, the Nederlandse Organisatie voor Wetenschappelijk Onderzoek (NWO), the Stichting voor Fundamenteel Onderzoek der Materie (FOM) and the Russian Foundation for Basic Research (RFBR) as well as the Dutch nanotechnology initiative NanoNed.

[5] Recently, we have managed to suppress dominating thermal effects in metallic GdFeCo and to observe true nonthermal effects of photons on spins [90].

References

[1] Kato Y, Myers R C, Gossard A C and Awschalom D D 2004 *Nature* **427** 50
[2] Ohno H, Chiba D, Matsukura F, Omiya T, Abe E, Dietl T, Ohno Y and Ohtani K 2000 *Nature* **408** 944
[3] Lottermoser T, Lonkai T, Amann U, Hohlwein D, Ihringer J and Fiebig M 2004 *Nature* **430** 541
[4] Asamitsu A, Tomioka Y, Kuwahara H and Tokura Y 1997 *Nature* **388** 50
[5] Yamanouchi Y, Chiba D, Matsukura F and Ohno H 2004 *Nature* **428** 539
[6] Beaurepaire E, Merle J C, Daunois A and Bigot J Y 1996 *Phys. Rev. Lett.* **76** 4250
[7] Bigot J Y, Guidoni L, Beaurepaire E and Saeta P N 2004 *Phys. Rev. Lett.* **93** 077401
[8] Hohlfeld J, Matthias E, Knorren R and Bennemann K H 1997 *Phys. Rev. Lett.* **78** 4861
[9] Güdde J, Conrad U, Jähnke V, Hohlfeld J and Matthias E 1999 *Phys. Rev.* B **59** R6608
[10] Scholl A, Baumgarten L, Jacquemin R and Eberhardt W 1997 *Phys. Rev. Lett.* **79** 5146
[11] Ju G, Nurmikko A V, Farrow R F C, Marks R F, Carey M J and Gurney B A 1999 *Phys. Rev. Lett.* **82** 3705
[12] Koopmans B, van Kampen M, Kohlhepp J T and de Jonge W J M 2000 *Phys. Rev. Lett.* **85** 844
[13] Rhie H S, Dürr H A and Eberhardt W 2003 *Phys. Rev. Lett.* **90** 247201
[14] Ogasawara T, Ohgushi K, Tomioka Y, Takahashi K S, Okamoto H, Kawasaki M and Tokura Y 2005 *Phys. Rev. Lett.* **94** 087202
[15] Bigot J Y 2001 *C. R. Acad. Sci. Ser.* IV *(Paris)* **2** 1483
[16] Hicken R J 2003 *Phil. Trans. R. Soc.* A **361** 2827
[17] Kimel A V, Kirilyuk A, Tsvetkov A, Pisarev R V and Rasing Th 2004 *Nature* **429** 850
[18] Astakhov G V, Kimel A V, Schott G M, Tsvetkov A A, Kirilyuk A, Yakovlev D R, Karczewski G, Ossau W, Schmidt G, Molenkamp L W and Rasing T 2005 *Appl. Phys. Lett.* **86** 152506
[19] Vomir M, Andrade L H F, Guidoni L, Beaurepaire E and Bigot J Y 2005 *Phys. Rev. Lett.* **94** 237601
[20] Ju G, Hohlfeld J, Bergman B, van de Veerdonk R J M, Mryasov O N, Kim J Y, Wu X, Weller D and Koopmans B 2004 *Phys. Rev. Lett.* **93** 197403
[21] Thiele J U, Buess M and Back C H 2004 *Appl. Phys. Lett.* **85** 2857
[22] Hohlfeld J, Gerrits Th, Bilderbeek M, Rasing Th, Awano H and Ohta N 2001 *Phys. Rev.* B **65** 012413
[23] Pitaevskii L P 1961 *Sov. Phys.—JETP* **12** 1008
[24] Pershan P S, van der Ziel J P and Malmstrom L D 1966 *Phys. Rev.* **143** 574
[25] van der Ziel J P, Pershan P S and Malmstrom L D 1965 *Phys. Rev. Lett.* **15** 190
[26] Deschamps J, Fitaire M and Lagoutte M 1970 *Phys. Rev. Lett.* **25** 001330
[27] Horovitz Y, Eliezer S, Ludmirsky A, Henis Z, Moshe E, Shpitalnik R and Arad B 1997 *Phys. Rev. Lett.* **78** 001707
[28] Ju G, Vertikov A, Nurmikko A V, Canady C, Xiao G, Farrow R F C and Cebollada A 1998 *Phys. Rev.* B **57** R700
[29] Bennet P J, Albanis V, Svirko Y P and Zheludev N I 1999 *Opt. Lett.* **24** 1373
[30] Wilks R, Kicken R J, Ali M, Hickey B J, Buchanan J D R, Pym A T G and Tanner B K 2004 *J. Appl. Phys.* **95** 7441
[31] Kimel A V, Bentivegna F, Gridnev V N, Pavlov V V, Pisarev R V and Rasing T 2001 *Phys. Rev.* B **63** 235201
[32] Melnikov A, Radu I, Bovensiepen U, Krupin O, Starke K, Matthias E and Wolf M 2003 *Phys. Rev. Lett.* **91** 227403
[33] Bovensiepen U, Melnikov A, Radu I, Krupin O, Starke K, Wolf M and Matthias E 2004 *Phys. Rev.* B **69** 235417
[34] Lisowski M, Loukakos P A, Melnikov A, Radu I, Ungureanu L, Wolf M and Bovensiepen U 2005 *Phys. Rev. Lett.* **95** 137402
[35] Oppeneer P M and Liebsch A 2004 *J. Phys.: Condens. Matter* **16** 5519
[36] Ohno H 1998 *Science* **281** 951
[37] Ohno H, Shen A, Matsukura F, Oiwa A, Endo A, Katsumoto S and Iye Y 1996 *Appl. Phys. Lett.* **69** 363
[38] Oiwa A, Mitsumori Y, Moriya R, Slupinski T and Munekata H 2002 *Phys. Rev. Lett.* **88** 137202
[39] Mitsumori Y, Oiwa A, Slupinski T, Maruki H, Kashimura Y, Minami F and Munekata H 2004 *Phys. Rev.* B **69** 033203
[40] Kimel A V, Astakhov G V, Schott G M, Kirilyuk A, Yakovlev D R, Karczewski G, Ossau W, Schmidt G, Molenkamp L W and Rasing Th 2004 *Phys. Rev. Lett.* **92** 237203
[41] Kojima E, Shimano R, Hashimoto Y, Katsumoto S, Iye Y and Kuwata-Gonokami M 2003 *Phys. Rev.* B **68** 193203
[42] Wang J, Sun C, Kono J, Oiwa A, Munekata H, Cywiński Ł and Sham L J 2005 *Phys. Rev. Lett.* **95** 167401
[43] Oiwa A, Takechi H and Munekata H 2005 *J. Supercond. Novel Mag.* **18** 9
[44] Wang J, Sun C, Hashimoto Y, Kono J, Khodaparast G A, Cywinski L, Sham L J, Sanders G D, Stanton C J and Munekata H 2006 *J. Phys.: Condens. Matter* **18** R501
[45] Kimel A V, Pisarev R V, Hohlfeld J and Rasing Th 2002 *Phys. Rev. Lett.* **89** 287401
[46] Zon B A and Kupershmidt V Y 1983 *Sov. Phys.—JETP* **57** 363

[47] Kovalenko V F and Nagaev E L 1986 *Sov. Phys. —Usp.* **29** 297
[48] Kabychenkov A F 1991 *Zh. Eksp. Teor. Fiz.* **100** 1219
Kabychenkov A F 1991 *JETP* **73** 672 (Engl. Transl.)
[49] Zvezdin A K and Kotov V A 1997 *Modern Magnetooptics and Magnetooptical Materials* (Bristol: IOP)
[50] Landau L D and Lifshitz E M 1984 *Theoretical Physics* vol 8 *Electrodynamics of Continuous Media* (Oxford: Pergamon)
[51] Pershan P S 1963 *Phys. Rev.* **130** 919
[52] Shen Y R and Bloembergen N 1966 *Phys. Rev.* **143** 372
[53] Zhang G P and Hübner W 2000 *Phys. Rev. Lett.* **85** 3025
[54] Gómez-Abal R, Ney O, Satitkovitchai K and Hübner W 2004 *Phys. Rev. Lett.* **92** 227402
[55] Kahn F J, Pershan P S and Remeika J P 1969 *Phys. Rev.* B **186** 891
[56] Wijn H P J 1994 *Numerical Data and Functional Relationships* (*Landolt–Bornstein New Series Group III*) vol 27f (Berlin: Springer)
[57] Dzyaloshinskii I E 1957 *Sov. Phys.—JETP* **5** 1259
[58] Moriya T 1960 *Phys. Rev.* **120** 91
[59] Usachev P A, Pisarev R V, Balbashov A M, Kimel A V, Kirilyuk A and Rasing Th 2005 *Phys. Status Solidi* **47** 2292
[60] Kimel A V, Kirilyuk A, Usachev P A, Pisarev R V, Balbashov A M and Rasing Th 2005 *Nature* **435** 655
[61] Shah J 1996 *Ultrafast Spectroscopy of Semiconductors and Semiconductor Nanostructures* (*Springer Series in Solid-State Sciences*) vol 115 (Berlin: Springer)
[62] Balbashov A M, Volkov A A, Lebedev S P, Mukhin A A and Prokhorov A S 1985 *Sov. Phys.—JETP* **61** 573
[63] Koshizuka N and Hayashi K 1988 *J. Phys. Soc. Japan* **57** 4418
[64] Kimel A V, Stanciu C D, Usachev P A, Pisarev R V, Gridnev V N, Kirilyuk A and Rasing T 2006 *Phys. Rev.* B **74** 060403R
[65] Perroni C A and Liebsch A 2006 *Phys. Rev.* B **74** 134430
[66] Kimel A V *et al* 2007 submitted
[67] Winkler G 1981 *Magnetic Garnets* (Braunschweig: Friedr. Vieweg & Sohn)
[68] Paoletti A (ed) 1978 *Physics of Magnetic Garnets* (*Enrico Fermi International School of Physics Italian Physical Society*) (Amsterdam: North-Holland)
[69] Hansteen F, Kimel A V, Kirilyuk A and Rasing Th 2005 *Phys. Rev. Lett.* **95** 047402
[70] Hansteen F, Kimel A V, Kirilyuk A and Rasing Th 2006 *Phys. Rev.* B **73** 014421
[71] Teale R W and Temple D W 1967 *Phys. Rev. Lett.* **19** 904
[72] Dillon J F, Gyorgy E M and Remeika J P 1969 *Phys. Rev. Lett.* **22** 643
[73] Alben R, Gyorgy E M, Dillon J F and Remeika J P 1972 *Phys. Rev.* B **5** 2560
[74] Chizhik A B, Davidenko I I, Maziewski A and Stupakiewicz A 1998 *Phys. Rev.* B **57** 14366
[75] Davidenko I, Maziewski A and Stupakiewicz A 1999 *J. Magn. Magn. Mater.* **196** 828
[76] Zaytseva I, Stupakiewicz A, Maziewski A and Zablotskii V 2003 *J. Magn. Magn. Mater.* **57** 254
[77] Veselago V G, Doroshenko R A and Rudov S G 1994 *Zh. Eksp. Teor. Fiz.* **105** 638
Veselago V G, Doroshenko R A and Rudov S G 1994 *JETP* **78** 341 (Engl. Transl.)
[78] Birss R R 1966 *Symmetry and Magnetism* (*Series of Monographs on Selected Topics in Solid State Physics*) 2nd edn (Amsterdam: North-Holland)
[79] Kalashnikova A M *et al* 2007 submitted
[80] Duong N P, Satoh T and Fiebig M 2004 *Phys. Rev. Lett.* **93** 117402
[81] Satoh T, Duong N P and Fiebig M 2006 *Phys. Rev.* B **74** 012404
[82] Perroni C A and Liebsch A 2006 *J. Phys.: Condens. Matter* **18** 7063
[83] Meier F and Zakharchenya B P (ed) 1984 *Optical Orientation* (*Modern Problems in Condensed Matter Sciences* vol 8) (Amsterdam: North-Holland)
[84] Awschalom D D, Warnock J and von Molnár S 1987 *Phys. Rev. Lett.* **58** 812
[85] Žutić I, Fabian J and Das Sarma S 2004 *Rev. Mod. Phys.* **76** 323
[86] Furdyna J K and Kossut J (ed) 1988 *Semiconductors and Semimetals* vol 25 *Diluted Magnetic Semiconductors* (New York: Academic)
[87] Akimoto R, Ando K, Sasaki F, Kobayashi S and Tani T 1998 *J. Appl. Phys.* **84** 6318
[88] Gupta J A, Knobel R, Samarth N and Awschalom D D 2001 *Science* **292** 2458
[89] Fernandez-Rossier J, Piermarocchi C, Chen P, MacDonald A H and Sham L J 2004 *Phys. Rev. Lett.* **93** 127201
[90] Stanciu C D *et al* 2007 submitted
[91] Hertel R 2006 *J. Magn. Magn. Mater.* **303** L1
[92] Keller U 2003 *Nature* **424** 831